

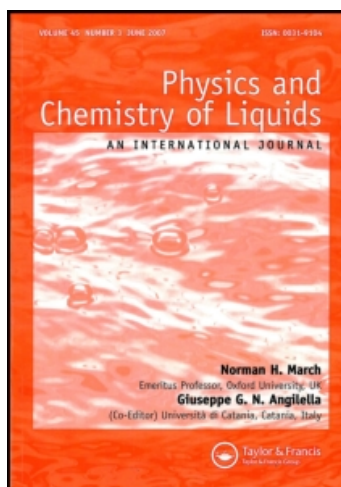
This article was downloaded by:

On: 28 January 2011

Access details: *Access Details: Free Access*

Publisher *Taylor & Francis*

Informa Ltd Registered in England and Wales Registered Number: 1072954 Registered office: Mortimer House, 37-41 Mortimer Street, London W1T 3JH, UK



Physics and Chemistry of Liquids

Publication details, including instructions for authors and subscription information:

<http://www.informaworld.com/smpp/title~content=t713646857>

The Solubility of Gases in Liquids

Jaime Wisniak^a; Alexander Apelblat^a; Hugo Segura^a

^a Department of Chemical Engineering, Ben-Gurion University of the Negev, Beer-Sheva, Israel

To cite this Article Wisniak, Jaime , Apelblat, Alexander and Segura, Hugo(1997) 'The Solubility of Gases in Liquids', *Physics and Chemistry of Liquids*, 34: 3, 125 — 153

To link to this Article: DOI: 10.1080/00319109708030558

URL: <http://dx.doi.org/10.1080/00319109708030558>

PLEASE SCROLL DOWN FOR ARTICLE

Full terms and conditions of use: <http://www.informaworld.com/terms-and-conditions-of-access.pdf>

This article may be used for research, teaching and private study purposes. Any substantial or systematic reproduction, re-distribution, re-selling, loan or sub-licensing, systematic supply or distribution in any form to anyone is expressly forbidden.

The publisher does not give any warranty express or implied or make any representation that the contents will be complete or accurate or up to date. The accuracy of any instructions, formulae and drug doses should be independently verified with primary sources. The publisher shall not be liable for any loss, actions, claims, proceedings, demand or costs or damages whatsoever or howsoever caused arising directly or indirectly in connection with or arising out of the use of this material.

THE SOLUBILITY OF GASES IN LIQUIDS

JAIME WISNIAK*, ALEXANDER APELBLAT
and HUGO SEGURA

*Department of Chemical Engineering Ben-Gurion University
of the Negev, Beer-Sheva, Israel*

(Received 13 November 1996)

The solubility of gases in liquids is analyzed in terms of the displacements theory, in particular the case where increasing solubility of gases is observed for rising temperature at room pressures. Heat effects are characterized for diluted binary mixtures and geometrical characteristics of phase envelopes (isopleths) are established. It is shown that gases which show increasing solubilities with temperature dissolve in heavy liquids by an endothermic process in the diluted range. A general approach, based on the analysis of critical lines and isopleths, is developed for all pressures and concentrations. It is demonstrated that increasing solubility will be observed if the isopleth of a liquid phase shows a nonmonotonous behavior. Conclusions and examples are illustrated using well-established cubic equations of state.

Keywords: Solubility of gases; azeotropy; equations of state; critical lines; phase envelopes

1. INTRODUCTION

In a recent communication Holmes [1] has made a qualitative analysis of the solubility of gases in liquids and pointed to the confusion present in general chemistry textbooks regarding the influence of temperature and the sign of the heat effect accompanying this phenomena. According to Holmes, some general chemistry textbooks affirm, directly or indirectly, the following:

- gases dissolve in liquids in an exothermic process,

*Corresponding author.

- a gas dissolved in a liquid always becomes less soluble with increasing temperature.

These facts are indeed observed in a large number of solubility data measured at room temperatures and ordinary pressures, but they cannot be considered as *general rules*. In particular, Holmes indicates that although it may difficult to rationalize, the experimental evidence shows that some gases become more soluble when temperature rises. In addition, he states that by Le Châtelier's Principle, under these conditions, the solubility process of a gas in a liquid *would be* an endothermic process. Unfortunately, no theoretical discussions accomplishing his deductions are presented. As with other thermodynamic phenomena, this particular case of gas solubility contradicts intuition and therefore a theoretical analysis allows to discern between a wrong interpretation based on poor experimental data and a rational interpretation based on thermodynamic facts.

It is our purpose to show that classical thermodynamics can be used to rationalize the temperature dependence of the solubility of gases in liquids and its calorimetric behavior.

2. THEORY

The theory of displacements was applied by Malesinski [2] to the study of azeotropy, based on this background it is possible to explain the change of the composition of the liquid phase when temperature is increased. We will first present a general overview of the displacements theory and the behavior of an intensive property when phase equilibrium conditions are assumed, and then apply these concepts specifically to the functionality of the solubility on temperature.

Phase equilibrium conditions for two species, distributed in two independent liquid-vapor phases, are met when:

$$\begin{aligned}\nabla P &= 0 \\ \nabla T &= 0 \\ \mu_i^L &= \mu_i^V \dots i = 1, 2\end{aligned}\tag{1}$$

where μ_i is the chemical potential of species i . Let us now suppose that an equilibrium state experiences an infinitesimal displacement in such

way that the system is allowed to achieve a new equilibrium state. From Eq. (1) we get:

$$\mu_i^L + d\mu_i^L = \mu_i^V + d\mu_i^V \Rightarrow d\mu_i^L = d\mu_i^V \quad (2)$$

Using classical thermodynamics the following differential relations for the chemical potential can be written for each component of a binary system [3]:

$$\begin{aligned} d\mu_1 &= -\bar{S}_1 dT + \bar{V}_1 dP + \left(\frac{\partial \mu_1}{\partial z_2} \right)_{T,P} dz_2 \\ d\mu_2 &= -\bar{S}_2 dT + \bar{V}_2 dP + \left(\frac{\partial \mu_2}{\partial z_2} \right)_{T,P} dz_2 \end{aligned} \quad (3)$$

where \bar{S}_i is the partial entropy, \bar{V}_i is the partial volume, and z_i is a generic composition (i.e., a liquid or a vapor phase composition). Since the Gibbs function is an extensive property its value for a single phase of a binary system is given by

$$\tilde{G} = z_1 \mu_1 + z_2 \mu_2 \quad (4)$$

Using Eq. (4) and the Gibbs-Duhem equation yields

$$\begin{aligned} \left(\frac{\partial^2 \tilde{G}}{\partial z_2^2} \right)_{T,P} &= \left(\frac{\partial \mu_2}{\partial z_2} \right)_{T,P} - \left(\frac{\partial \mu_1}{\partial z_2} \right)_{T,P} \\ &= -\frac{1}{z_2} \left(\frac{\partial \mu_1}{\partial z_2} \right)_{T,P} = \frac{1}{1-z_2} \left(\frac{\partial \mu_2}{\partial z_2} \right)_{T,P} \end{aligned} \quad (5)$$

Replacement of Eq. (5) in Eq. (3), yields:

$$d\mu_1 = -\bar{S}_1 dT + \bar{V}_1 dP - z_2 \left(\frac{\partial^2 \tilde{G}}{\partial z_2^2} \right)_{T,P} dz_2 \quad (6)$$

$$d\mu_2 = -\bar{S}_2 dT + \bar{V}_2 dP + (1-z_2) \left(\frac{\partial^2 \tilde{G}}{\partial z_2^2} \right)_{T,P} dz_2 \quad (7)$$

For a two-phase binary equilibrium, like vapor-liquid equilibrium (VLE), Eqs. (6) and (7) can be applied to each component in each

phase and the following relations can be obtained from Eq. (2):

$$-\Delta\bar{S}_1 dT + \Delta\bar{V}_1 dP - y_2 \left(\frac{\partial^2 \tilde{G}^v}{\partial y_2^2} \right)_{T,P} dy_2 + x_2 \left(\frac{\partial^2 \tilde{G}^L}{\partial x_2^2} \right)_{T,P} dx_2 = 0 \quad (8)$$

$$\begin{aligned} -\Delta\bar{S}_2 dT + \Delta\bar{V}_2 dP + (1 - y_2) \left(\frac{\partial^2 \tilde{G}^v}{\partial y_2^2} \right)_{T,P} \\ dy_2 - (1 - x_2) \left(\frac{\partial^2 \tilde{G}^L}{\partial x_2^2} \right)_{T,P} dx_2 = 0 \end{aligned} \quad (9)$$

In Eqs. (8) and (9) $\Delta\bar{S}_i = \bar{S}_i^v - \bar{S}_i^L$ is the partial entropy of vaporization and $\Delta\bar{V}_i = \bar{V}_i^v - \bar{V}_i^L$ is the partial volume of vaporization. Eliminating $(\partial^2 \tilde{G}^L / \partial x_2^2)_{T,P}$ from Eqs. (8) and (9) yields:

$$\begin{aligned} -(y_1 \Delta\bar{S}_1 + y_2 \Delta\bar{S}_2) dT + (y_1 \Delta\bar{V}_1 + y_2 \Delta\bar{V}_2) dP \\ + (x_2 - y_2) \left(\frac{\partial^2 \tilde{G}^L}{\partial x_2^2} \right)_{T,P} dx_2 = 0 \end{aligned} \quad (10)$$

Constraining Eq. (10) to constant pressure yields the following expression for the variation of solubility with temperature:

$$\left(\frac{\partial x_2}{\partial T} \right)_P = - \left(\frac{\partial x_1}{\partial T} \right)_P = \frac{y_1 \Delta\bar{S}_1 + y_2 \Delta\bar{S}_2}{(x_2 - y_2)} \left(\frac{\partial^2 \tilde{G}^L}{\partial x_2^2} \right)_{T,P}^{-1} \quad (11)$$

Equation 11 is completely general for binary systems in VLE, it contains the second compositional derivative of the Gibbs energy in the liquid phase which must be positive for stable liquid compositions [3]. At constant temperature and pressure we have:

$$\Delta\bar{S}_i = \frac{\Delta\bar{H}_i}{T} \quad (12)$$

Let us now assume that component 1 is the most volatile component. Combination of Eqs. (11) and (12) yields:

$$\left(\frac{\partial x_1}{\partial T} \right)_P = - \frac{y_1 \Delta\bar{H}_1 + y_2 \Delta\bar{H}_2}{T(y_1 - x_1)} \left(\frac{\partial^2 \tilde{G}^L}{\partial x_2^2} \right)_{T,P}^{-1} \quad (13)$$

Inspection of Eq. (13) indicates that the sign of its left hand side is given by the sign of the sum $y_1 \Delta\bar{H}_1 + y_2 \Delta\bar{H}_2$. This relation is

remarkable because *no approximations* have been made in its derivation and because it relates the change in solubility with temperature with the enthalpy of vaporization of the mixture. Generally, at low pressure conditions and when nonsupercritical components are present, the partial enthalpy is positive and of the order of magnitude of the pure component vaporization enthalpy. Thus if no azeotrope is present, it is clear that the solubility of the most volatile component *decreases* when temperature is *increased*.

From a calorimetric viewpoint Eq. (13) can be used to obtain some important conclusions about the enthalpy effect of the solubility process, as illustrated below for subcritical and supercritical systems.

1. Subcritical systems with azeotropic behavior

A subcritical system is defined as a mixture whose components are at reduced temperatures, $T_r = T/T_c$, smaller or equal than the unity. As a particular example, consider the system 2-propanone (1) – trichloromethane (2) for which experimental vapor-liquid equilibrium at 101.325 kPa (Fig. 1) and heats of mixing data at two temperatures (Fig. 2) are available [4, 5, 6]. Both sets of data can be used to

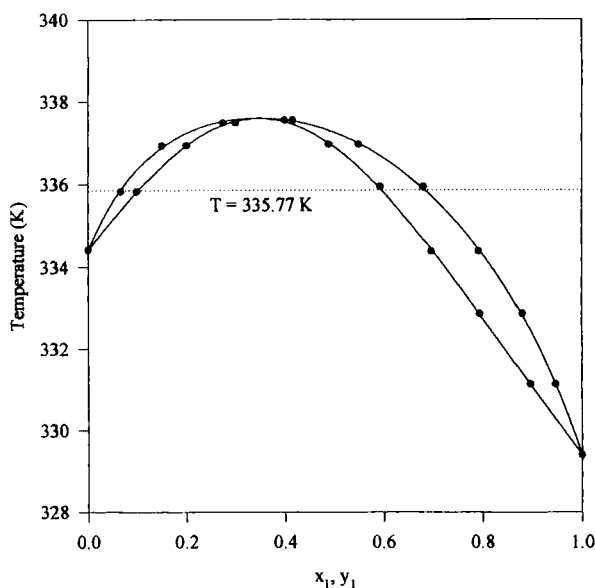


FIGURE 1 Phase equilibrium diagram for the 2-propanone (1) – trichloromethane (2) system. Experimental data of Kudryavtseva and Susarev⁴.

construct the corresponding enthalpy - concentration diagram (Fig. 3). Inspection of Figure 1 shows that the system forms a maximum temperature azeotrope of composition $x_1 \approx 0.36$. For compositions less than the azeotropic one the solubility of the most volatile component (2-propanone) increases in the liquid phase when temperature increases. As can be seen in Figure 2, the UNIFAC method [7] shows a good agreement with the experimental excess enthalpy data, allowing a reliable extrapolation of the enthalpy in the range of the system boiling temperatures. Furthermore, it is concluded that at 101.325 kPa the solubility process is exothermic for the whole range of liquid-phase equilibrium compositions and temperatures. To illustrate the temperature and solubility behaviour of this type of systems, suppose we want to determine the heat effect involved in the solubility process to form a solution in VLE with a liquid phase composition $x_1 = 0.1$. As seen from Figure 1, this composition falls in the range where the solubility of the most volatile component in the liquid phase increases when temperature is increased. From Figure 1 we get that the pertinent equilibrium temperature and pressure are 335.77 K and 101.325 kPa respectively; under these conditions pure 2-

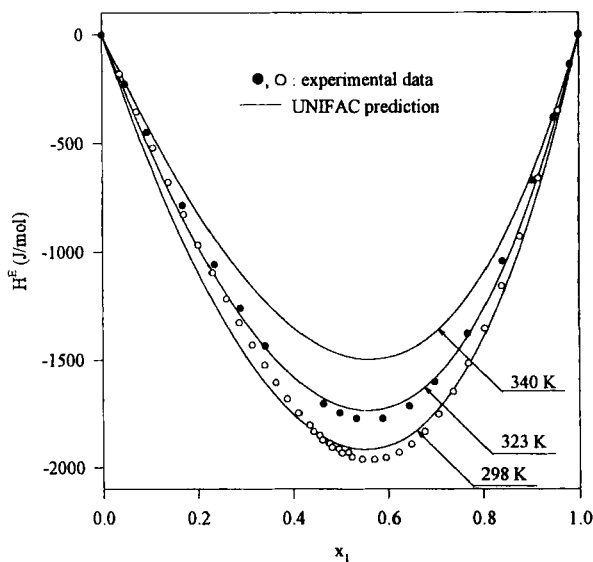


FIGURE 2 Excess enthalpy for the 2-propanone (1) - trichloromethane (2) system. Experimental data of Becker and Hallauer⁵ at 298.15 K and of Morris *et al.*⁶ at 323.15 K.

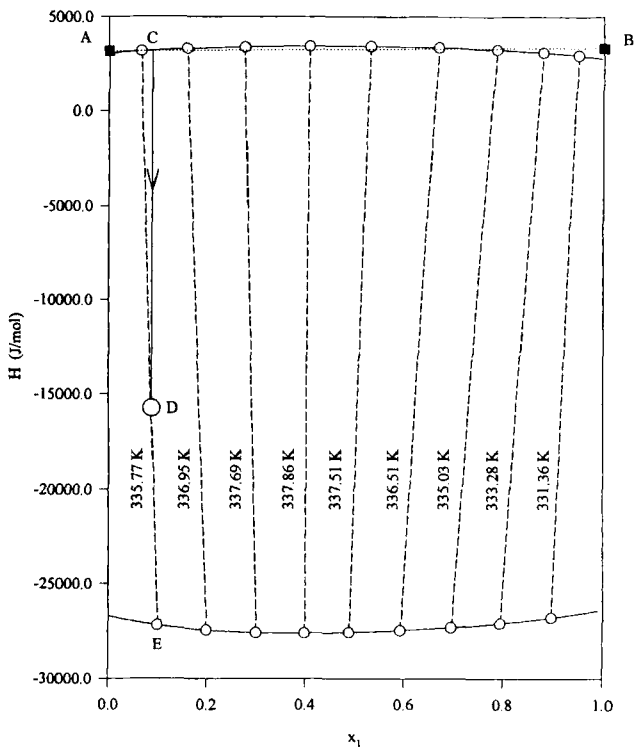


FIGURE 3 Enthalpy – composition diagram for the 2-propanone (1) – trichloromethane (2) system at 101.325 kPa.

propanone (point A) and pure trichloromethane (point B) are superheated vapors, but if they are mixed then there is a compositional range CD where *condensation will occur with the corresponding release of heat*. If we refer now to Figure 3 points A and B indicate the enthalpy of pure 2-propanone and pure trichloromethane respectively, at atmospheric pressure and 335.77 K. Line AB represents the energy balance when these components are mixed adiabatically. To form a vapor-liquid equilibrium mixture with composition D, at the same temperature and pressure of the constituents, heat must evolve from the system to its surroundings in an amount equivalent to the segment CD per mole of solution formed. Clearly then, the heat effect of the solubility process must qualified as *exothermic*. In the case in question the increase of solubility of the most volatile component with temperature cannot be explained in terms of *an endothermic* solubility

process, but in terms of the *inversion* of relative volatilities at the azeotropic point. Thus qualification of a solubility process as being endothermic or exothermic is not clear cut. For the system under consideration we see that up to the azeotropic composition the solubility of the more volatile component will increase with an increase in temperature, but after the azeotropic composition the solubility will *decrease* with an increase in temperature. Azeotropy is a common enough phenomena to justify the statement that solubility may increase with an increase in temperature depending on the position of the azeotrope and its deviation from ideality. Solubility increases with temperature when the composition of the volatile component is lower than the maximum boiling point azeotropic composition. For systems with minimum boiling points azeotropes, solubility increases when the composition of the volatile component is greater than the azeotropic composition.

The important points to be learned from this simple illustration are:

- according to Eq. (13), the derivative of the solubility with temperature depends on the sign of the partial vaporization enthalpies and on the sign of the difference $(y_1 - x_1)$. Hence, if no azeotrope exists and the sum $y_1\Delta\bar{H}_1 + y_2\Delta\bar{H}_2$ is negative, then the solubility of the more volatile species will increase with an increase in temperature.
- the sum $y_1\Delta\bar{H}_1 + y_2\Delta\bar{H}_2$ (heat of vaporization) should not be confused with the heat effect of the process. In the example given above this sum is always positive and although, in general, positive vaporization enthalpies are related to *endothermic* processes the solubility process for increasing solubility of the most volatile component will be *exothermic*, as we have demonstrated. The correct qualification of the heat effect of this process (endothermic or exothermic) must be deduced from an energy balance. Appendix A illustrates the energy balance for the solubility of gases in practically nonvolatile solvents.

2. Binary systems with nonvolatile solvents and supercritical gases

Azeotropic behavior is not observed when practically nonvolatile solvents are mixed with supercritical gases at low pressures. In these systems the gas component is concentrated in the vapor phase and the

following reasonable approximations can be made:

- the composition of the nonvolatile solvent in the vapor phase is negligible ($y_2 \approx 0$).
- the solubility of the gaseous (supercritical) component in the liquid phase is low compared to that of the nonvolatile component ($x_1 \approx 0$).

Introducing these assumptions Eq. (13) becomes

$$\left(\frac{\partial x_1}{\partial T}\right)_P = -\frac{y_1 \Delta \bar{H}_1 + y_2 \Delta \bar{H}_2}{T(y_1 - x_1)} \left(\frac{\partial^2 \tilde{G}^L}{\partial x_2^2}\right)_{T,P}^{-1} \approx -\frac{\Delta \bar{H}_1}{T} \left(\frac{\partial^2 \tilde{G}^L}{\partial x_2^2}\right)_{T,P}^{-1} \quad (14)$$

The Gibbs function of the liquid phase for a binary mixture can be written as

$$\tilde{G}^L = \tilde{G}^E + \sum_{i=1}^2 x_i \tilde{G}_i^{\text{ideal}} \quad (15a)$$

with

$$\tilde{G}^E = RT(\ln \gamma_1 + \ln \gamma_2) \quad (15b)$$

$$\tilde{G}_i^{\text{ideal}} = RT \ln x_i + \tilde{G}_i^0(T, P) \quad (15c)$$

where \tilde{G}_i^0 is a reference value that depends only on temperature and pressure. From Eqs. (15) it follows that:

$$\left(\frac{\partial^2 \tilde{G}^L}{\partial x_2^2}\right)_{T,P} = \left(\frac{\partial^2 \tilde{G}^E}{\partial x_2^2}\right)_{T,P} + \frac{RT}{x_1 x_2} = \frac{\partial \ln \gamma_2}{\partial x_2} - \frac{\partial \ln \gamma_1}{\partial x_2} + \frac{RT}{x_1 x_2} \quad (16)$$

Since it has been assumed that the gas component has a low solubility the second term of the right member of Eq. (16) is dominant because the compositional derivative of the activity coefficients in the liquid is always finite, even in the diluted ranges. Thus taking into consideration that as $x_1 \rightarrow 0$ ($x_2 \rightarrow 1$), $\gamma_1 \rightarrow \gamma_1^\infty$ and $\gamma_2 \rightarrow 1$, we can approximate Eq. (16) by

$$\left(\frac{\partial^2 \tilde{G}^L}{\partial x_2^2}\right)_{T,P,x_1 \rightarrow 0} \approx \frac{RT}{x_1} \quad (17)$$

Replacement of Eq. (17) in Eq. (14) yields:

$$\left(\frac{\partial x_1}{\partial T}\right)_{P, x_1 \rightarrow 0} \approx -\frac{x_1 \Delta \bar{H}_1}{RT^2} \quad (18)$$

From Eq. (18) it is clear that the temperature slope of the solubility at constant pressure depends only on the sign of $-\Delta \bar{H}_1$ which is equal to the sign of the heat effect of the gas solubility in a nonvolatile liquid, as shown in Appendix A. Thus if the solubility increases with temperature, the partial vaporization enthalpy will be negative and the observed heat effect *will be endothermic* provided that the assumptions involved in Eq. (18) are applicable.

Following the reasoning of Prausnitz *et al.* [8], the partial enthalpy of the supercritical component can be written as

$$\Delta \bar{H}_1 = \bar{H}_1^v(y_1 \rightarrow 1) - \bar{H}_1^L(x_1) \approx \tilde{H}_1^v - \tilde{H}_1^L - (\bar{H}_1^L(x_1) - \tilde{H}_1^L) \quad (19)$$

where \tilde{H}_1^L is the enthalpy of a liquid phase which contains pure component 1. It must be understood that if component 1 is supercritical, then \tilde{H}_1^L represents the enthalpy of an *hypothetical* liquid phase because at the equilibrium conditions 1 cannot exist as a pure liquid. From Eq. (19) it is deduced that the partial enthalpy of the gas component is composed of the contribution of a hypothetical vaporization enthalpy ($\tilde{H}_1^v - \tilde{H}_1^L$) and a partial excess (or mixing) enthalpy ($\bar{H}_1^L(x_1) - \tilde{H}_1^L$). If solubility increases with temperature then $\Delta \bar{H}_1$ must be negative as can be deduced from Eq. (18); if the vaporization enthalpy is positive then the partial excess enthalpy will be positive yielding a negative sign for the partial enthalpy of component 1 in Eq. (19).

Once again we see that the conclusions discussed in the preceding paragraph deserve a careful analysis because, as pointed by Prausnitz *et al.* [8], the gas vaporization enthalpy (an hypothetical quantity) can be negative and may not be treated as a subcritical compound vaporization enthalpy, which is always positive.

3. Prediction of solubility of gases in liquids using equations of state

An equation of state (EOS) may be used for predicting the variation of the solubility of a gas with temperature. As an example, we will use the van der Waals EOS for the prediction of increased gas solubility with rising temperature. The limitations of the van der Waals theory are

well known, but as has been pointed Van Konynenburg and Scott [9], it very rarely yields physically absurd results. The use this EOS will be illustrated with the system hydrogen (1) – water (2) for which an increasing solubility behavior has been reported by Wild *et al.* [10] in the range of atmospheric pressure. Figure 4 shows the gas solubility of the mixture in question, as predicted by van der Waals' EOS and calculated using the relation [11]:

$$\hat{f}_i^L = \hat{f}_i^V \Rightarrow x_i \hat{\phi}_i^L = y_i \hat{\phi}_i^V \quad (20)$$

where \hat{f}_i and $\hat{\phi}_i$ are the fugacities and fugacity coefficients of component i in both phases (L and V). The fugacity coefficient for a pressure-explicit EOS, as the van der Waals EOS, can be calculated as follows [11]:

$$\ln \hat{\phi}_i = \frac{1}{RT} \int_{\tilde{v}}^{\infty} \left[\left(\frac{\partial P}{\partial n_i} \right)_{T, n\tilde{v}, n_j} - \frac{RT}{\tilde{V}} \right] d\tilde{V} - \ln \frac{P\tilde{V}}{RT} \quad (21)$$

Pure component critical properties have been taken from Reid *et al.* [12] and no interaction parameters have been introduced in the

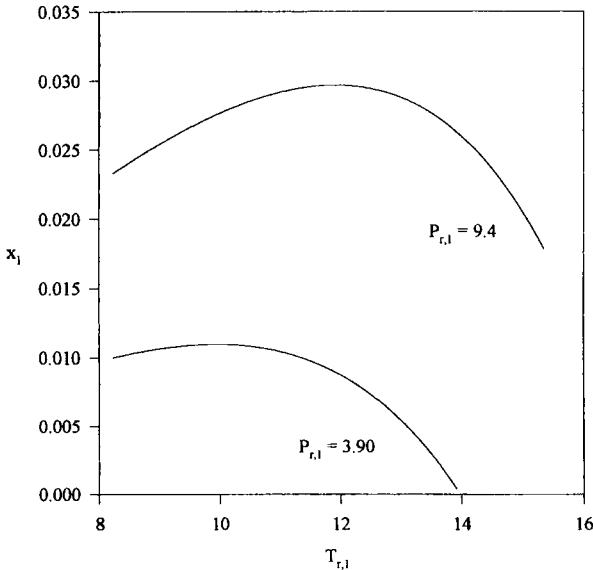


FIGURE 4 Prediction of increasing gas solubilities with van der Waals equation of state.

mixing rules. Figure 4 shows that although van der Waals equation does not predict the increase in solubility observed in the range of atmospheric pressure ($P_{r,1} = P/P_{c,1} = 7.8 \times 10^{-2}$), it does so at higher pressures. From a qualitatively viewpoint, these results are remarkable because no parameters other than critical properties have been used.

On the basis of the van der Waals EOS, it is possible to discuss the problem on a wider basis by studying the critical lines of the mixtures under consideration. Mixtures which exhibit increasing solubility with temperature for the gas component are characterized by large differences in the critical properties of the constituents. Following the classification of Van Konynenburg and Scott [9] mixtures of this nature are classified as systems of type III. Figure 5a shows a qualitative P-T projection of the critical lines for a mixture of this type (the Figure corresponds to a detailed calculation under the conditions of the Figure 16 in the work of Van Konynenburg and Scott [9], where $\zeta = 0.565$ and $\Lambda = 0.0869$). See the original reference for nomenclature. Properties have been reduced in terms of the critical properties of the

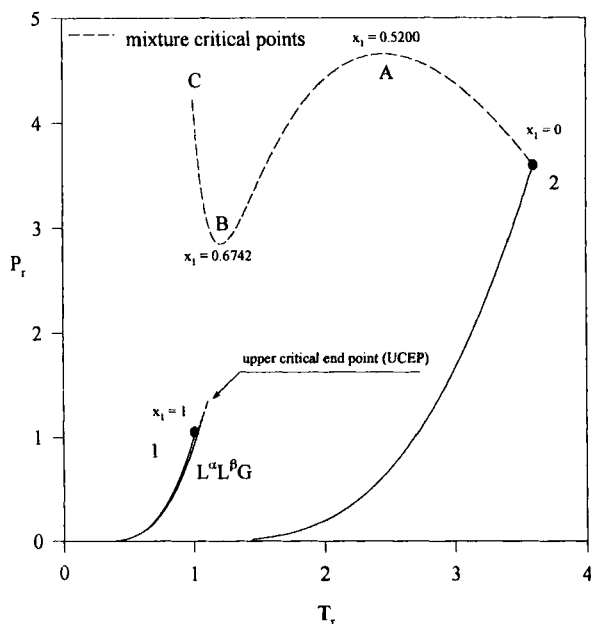


FIGURE 5a P-T projections of critical lines for a system type III ($\zeta = 0.565$ and $\Lambda = 0.0869$).

gas component, denoted by 1). As seen from the figure, systems of type III are characterized by critical liquid-gas lines which do not connect the critical points of pure compounds; one branch of the critical line emerges from the light component 1 and ends in an upper critical end point (UCEP) yielding a common intersection with a three phase line ($L^\alpha L^\beta G$), the other branch (2ABC) emerges from the critical point of the heavy component 2 and moves towards the range of high pressures. The critical lines generated by the van der Waals EOS are comparable with those found experimentally, examples of the critical projections shown in Figure 5a are the systems ethane + methanol, carbon dioxide + hexadecane, methane + methylcyclopentane [13], methane + n-heptane [14], further experimental evidence is discussed by Hicks and Young [15].

The pertinent $x - T$ and $x - P$ projections of the critical line 2ABC shown in Figure 5a are plotted in Figure 5b. Of particular interest is the minimum pressure present at point B, because in its neighborhood the composition of the critical liquid-gas point goes through a maximum value. In addition, critical points are enriched in component 1 for increasing temperatures from C to the maximum in composition, in the range of pressures and temperatures which is below the critical pressure of the heavy component (2) and above the critical temperature of the light component (1). The above discussion corresponds to the experimentally observed cases of increasing gas solubility where the behavior discussed appears in ranges in which the solvent is subcritical and the solute is supercritical. To clarify this point further, let us consider the binary VLE diagram related to systems of type III, which is shown in Figure 5c, for a wide range of reduced pressures (the pertinent Figure corresponds to the specifications considered in Figure 5a). Figure 5c displays the vapor-liquid isotherms which will be observed in the neighborhood of reduced temperatures of the minimum point B; isotherms which are located below the indicated UCEP are those which emerge from component 1 (in Figure 5a) and the others are isotherms which meet critical points in the line 2ABC. In Figure 5c two facts are clearly depicted: (a) For the set of isotherms below UCEP (considering line DE) the solubility of the light component decreases with increasing temperature, which is the familiar case, (b) For the set of isotherms above UCEP (considering line FG) the solubility of the light component increases with increasing temperature. In addition, the pressure of the critical point decreases with increasing temperatures due to the minimum in pressure given by point B in Figure 5a.

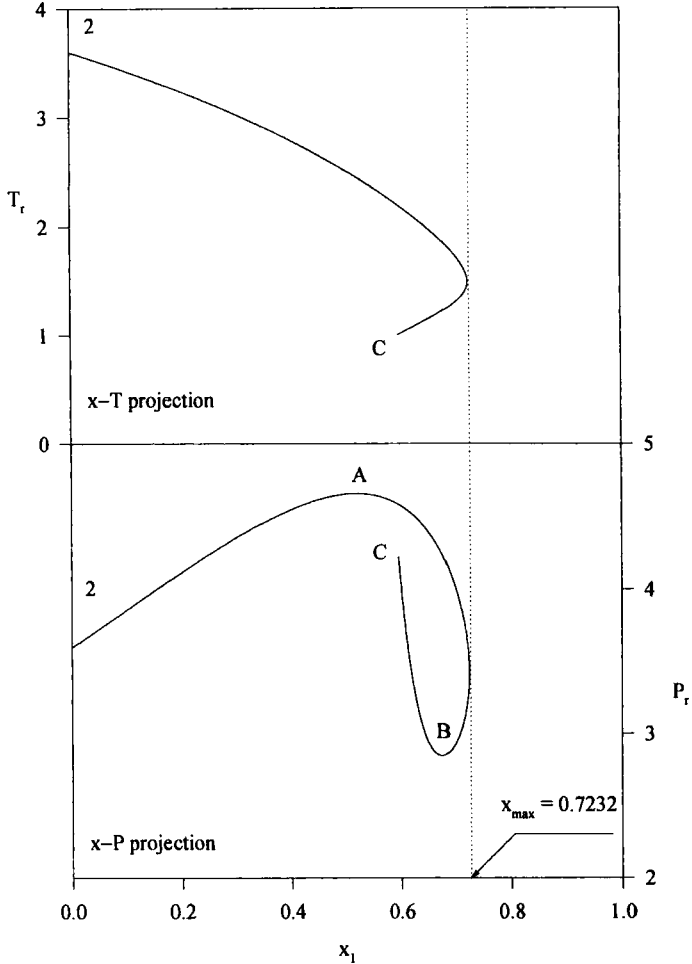


FIGURE 5b x - T and x - P projections for the critical lines in Figure 5a.

However, not every system of type III presents the minimum value of the pressure in its critical lines shown in Figure 5a, which has been used for explaining increasing solubilities. Some possible variations of critical lines for systems type III are shown in Figure 5d, and occur fundamentally in the critical line that emerges from component 2. Using the classification of gas-gas equilibria given by Schneider [13] we can say that line 2C' generates systems of type III with gas-gas

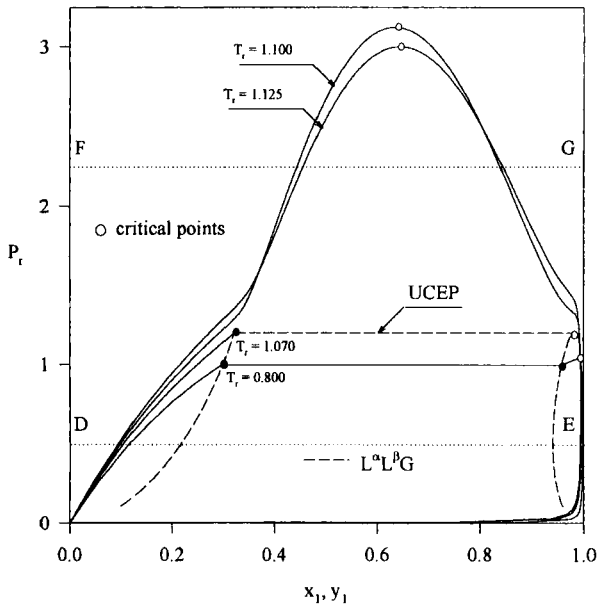


FIGURE 5c Phase equilibrium diagram for the system illustrated in Figure 5a.

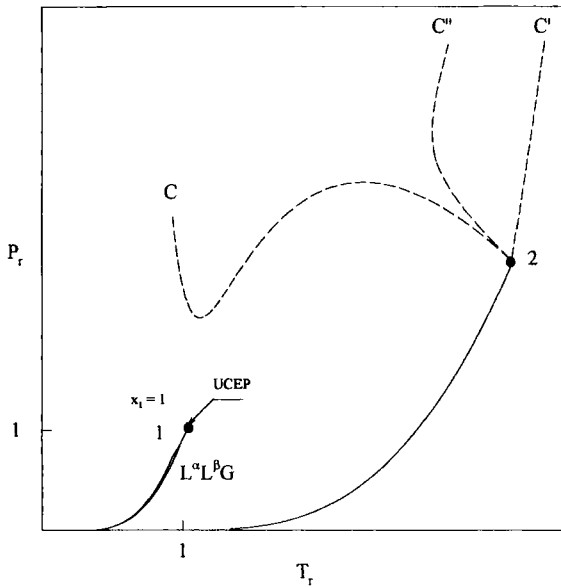


FIGURE 5d General P-T projections of critical lines for a system type III.

equilibria of the first type and line 2C'' originates systems of type III with gas-gas equilibria of the second type; experimental examples of these behavior are the systems argon + water (first type) and nitrogen + water (second type). The aforementioned systems present also increasing solubilities with increasing temperatures at room pressures [8]. A more detailed explanation of this behavior may be obtained by studying the isopleths (lines of constant composition in noncritical equilibrium states, also called phase envelopes). To do so we will first develop general relations for the isopleths using the displacement theory presented before. Equation (10) constrained to constant liquid composition yields

$$\left(\frac{\partial P}{\partial T}\right)_{x_2} = \frac{y_1 \Delta \bar{S}_1 + y_2 \Delta \bar{S}_2}{y_1 \Delta \bar{V}_1 + y_2 \Delta \bar{V}_2} \quad (22)$$

which combined with Eq. (12) gives the following

$$\left(\frac{\partial P}{\partial T}\right)_{x_2} = \frac{y_1 \Delta \bar{H}_1 + y_2 \Delta \bar{H}_2}{T(y_1 \Delta \bar{V}_1 + y_2 \Delta \bar{V}_2)} = \frac{\Omega_{yh}}{T\Omega_{yv}} \quad (23)$$

Equation (23) is a Clapeyron-type relation for binary mixtures and can be used to analyze the influence of the temperature on the bubble-point, at constant composition. A similar relation can be obtained for the variation of the dew-point pressure with temperature [2]

$$\left(\frac{\partial P}{\partial T}\right)_{y_2} = \frac{x_1 \Delta \bar{H}_1 + x_2 \Delta \bar{H}_2}{T(x_1 \Delta \bar{V}_1 + x_2 \Delta \bar{V}_2)} = \frac{\Omega_{xh}}{T\Omega_{xv}} \quad (24)$$

Figure 6a shows the isopleth of global composition 0.63 for the example illustrated in Figure 5a. This particular value of the composition is suggested by Figure 5c where increasing solubilities with temperature are observed above the UCEP. The dew-point segment of the isopleth (extending from *D* to CPI) represents the geometrical P-T (P-T) locus where a vapor of constant composition ($y_2 = 0.63$) is in equilibrium with a liquid phase. The segment in question ends at the critical point CPI where continuity with a liquid phase of the same composition is achieved. From point CPI on the isopleth represents now a liquid phase of constant composition

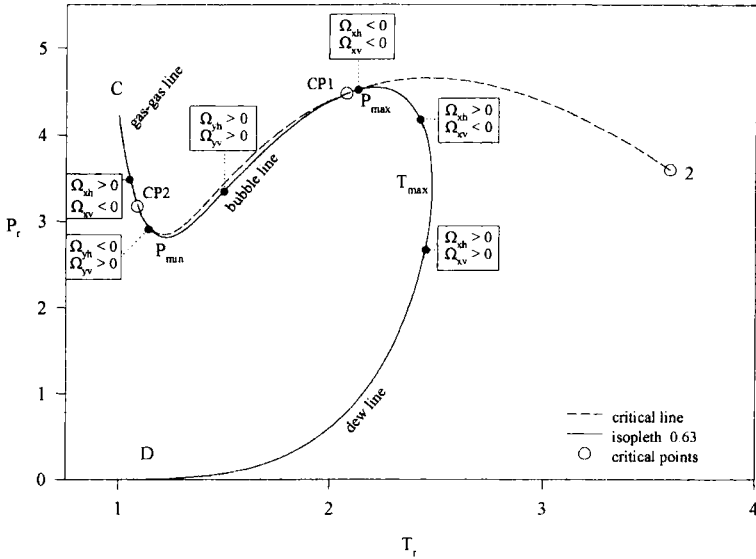


FIGURE 6a Isopleth of composition 0.63 for a mixture type III ($\zeta = 0.565$ and $\Lambda = 0.0869$).

($x_1 = 0.63$) which extends until a second critical point (CP2) is reached. Each critical point along an isopleth implies a change of phase of constant composition. In addition, every extreme point along the isopleth indicates that the value of the numerator or the denominator in Eq. (23) or (24) becomes zero depending on the phase present at the particular extreme point. Let us now analyze the slope of the dew line extending from D to CP1. Starting from point D, located in the low pressure range where partial vaporization properties are positive ($\Omega_{xh} > 0$ and $\Omega_{xv} > 0$), the slope of the isopleth is observed to be positive in agreement with Eq. (24). This segment presents a maximum temperature (T_{max}) where the isopleth has an infinite slope. According to Eq. (24) this maximum requires that Ω_{xv} be zero. From thereon the slope becomes negative which necessarily implies that the sign of Ω_{xv} has changed from a positive value to a negative one. The following segment of the curve has a negative slope ($\Omega_{xh} > 0$ and $\Omega_{xv} < 0$ in Eq. (24) and presents a second extreme point (P_{max}) which can be explained by a zero value in Ω_{xh} . Thereafter Ω_{xh} changes its sign from positive to negative. From the maximum pressure the curve reaches the critical point CP1 with a positive slope ($\Omega_{xh} < 0$ and $\Omega_{xv} < 0$ in Eq. (24). In the neighborhood of critical points, where

phases are indistinguishable, the signs of Ω_{zm} for different phases are opposite as a consequence of the fact that in binary systems phases meet a critical point with opposite pressure (or temperature) slopes, as can be clearly seen in the high pressure range of Figure 5b (a demonstration is presented in Appendix B). Hence, in the immediate neighborhood of point CP1, and on the bubble-point pressure segment, Ω_{yh} and Ω_{yv} are both positive, yielding a positive slope of the isopleth, as evident in the figure and in concordance with Eq. (23). The bubble-point pressure segment (extending from CP1 to CP2) passes through a point of minimum pressure where Ω_{yh} becomes zero with Ω_{yv} positive. From the minimum pressure point on, p_{\min} , Ω_{yh} changes its sign from positive to negative and the bubble-point pressure segment ends at the critical point CP2, with a negative slope, explained again by Eq. (23). The negative slope for the segment CP2-C is easily deduced by following the rules of changes of sign in the critical slope. The geometric characteristics of Figure 6a have been summarized in Table I.

The rules discussed above, regarding the changes of sign of Ω_{zm} , can be generalized as follows:

1. An extreme value of the pressure implies a change of sign in Ω_{zh} , where z is the composition of the phase in equilibrium with the fixed composition phase represented by the isopleth.
2. An extreme value of the temperature implies a change of sign in Ω_{zv} , where z is the composition of the phase in equilibrium with the fixed composition phase represented by the isopleth.

TABLE I Summary of geometrical characteristics for the isopleth in Figure 6a

Range	Phase	Ω_{xh} Eq. (24)	Ω_{yv} Eq. (24)	Ω_{yh} Eq. (23)	Ω_{yv} Eq. (23)	$(\frac{\partial P}{\partial T})$
D – T _{max}	vapor	+	+	---	---	+
T _{max}	vapor	+	0	---	---	∞
T _{max} – P _{max}	vapor	+	–	---	---	–
P _{max}	vapor	0	–	---	---	0
P _{max} – CP1	vapor	–	–	---	---	+
CP1	vapor/liquid	0	0	0	0	+
CP1 – P _{min}	liquid	---	---	+	+	+
P _{min}	liquid	---	---	0	+	0
P _{min} – CP2	liquid	---	---	–	+	–
CP2	liquid/gas	0	0	0	0	–
CP2-C	gas	+	–	---	---	–

3. A critical point implies a change of the phase which is represented by the isopleth at constant sign of slope, in addition both Ω_{zh} and Ω_{zv} will change their signs from left to the right neighborhood of the critical point. As before, z is the composition of the phase in equilibrium with the fixed composition phase represented by the isopleth.

The rules presented above are valid *both* for experimental or simulated cases, because they are a consequence of the displacement theory expressed by Eqs. (23) and (24). Our analysis is based on EOS because little experimental information is available regarding isopleths. It should be pointed, however, that phase envelopes generated by cubic EOS represent the experimental behavior with an excellent qualitative agreement, and these predictions are useful for the analysis of retrograde behavior. Following the general rules, and from an inspection of Eqs. (14) and (23), we can deduce that every stationary point in pressure along an isopleth corresponding to a liquid phase (bubble-point pressure segments) has a direct influence in the solubility, this is because *both equations contain the same enthalpic term* Ω_{yh} . Combination of Eqs. (14) and (23) yields

$$\left(\frac{\partial x_1}{\partial T}\right)_p = -\frac{\Omega_{yv}}{y_1 - x_1} \left(\frac{\partial P}{\partial T}\right)_{x_2} \left(\frac{\partial^2 \tilde{G}^L}{\partial x_2^2}\right)_{T,P}^{-1} \quad (25)$$

Equation (25) shows clearly that *every extreme in pressure along the bubble line of an isopleth implies an extremal point in solubility*. Selecting 1 as the light component, the difference $(y_1 - x_1)$ is positive and, remembering that the second compositional derivative of the Gibbs energy is positive as was discussed before, it is concluded that the sign of the concavity of the extremal point in solubility will be opposite to the sign of the concavity of the extreme point in pressure if Ω_{yv} is positive, or both concavities have the same sign if Ω_{yv} is negative. In the example presented in Figure 6a, the minimum pressure of the isopleth between CP1 and CP2 implies a maximum of the solubility in temperature and, obviously, solubility increases with rising temperature between CP2 and P_{\min} . This behavior is depicted in Figure 5c, above the UCEP, in the reference line F-G.

On the basis of the rules discussed above and Eq. (25), further cases of increasing solubility of the light component with rising temperature

can be illustrated. Figure 6b shows (schematically) an isopleth where the critical point is located between the maximum pressure and the maximum temperature, in this case the behavior appears in the retrograde region between the critical point and the maximum pressure. The case of increasing solubility considered in Figure 6b is common when the slope of the critical line is negative because the isopleth will meet the critical line tangentially at the critical point. Figure 6c shows the case where the slope of the critical line is negative, in this case both the maximum temperature and pressure are observed to occur *above* the critical point in the bubble-pressure segment of the isopleth. Once again, a range of increasing solubilities appears, but now it is inside the range of maximum pressure and the maximum temperature. Note that the behavior of increasing solubilities of the light component with rising temperature takes place ordinarily in the retrograde region and is related to a negative vaporization enthalpy. In addition, this behavior will usually appear in ranges where the slope of the isopleth in the bubble line segment is negative because the

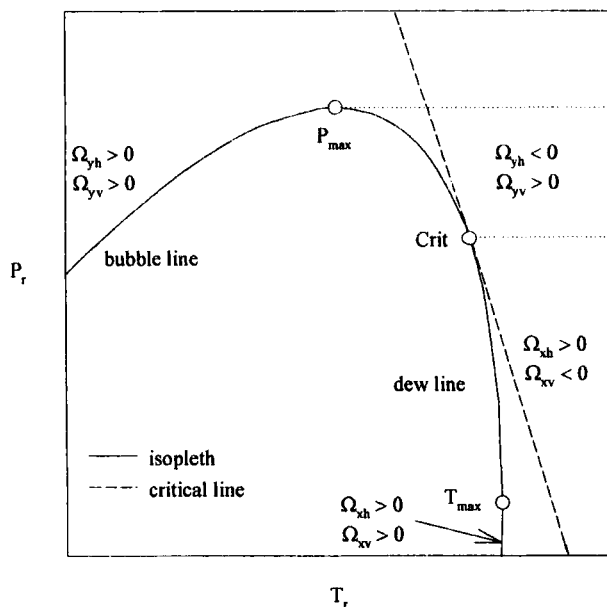


FIGURE 6b Schematic isopleth where the critical point is located between the maximum temperature and the maximum pressure.

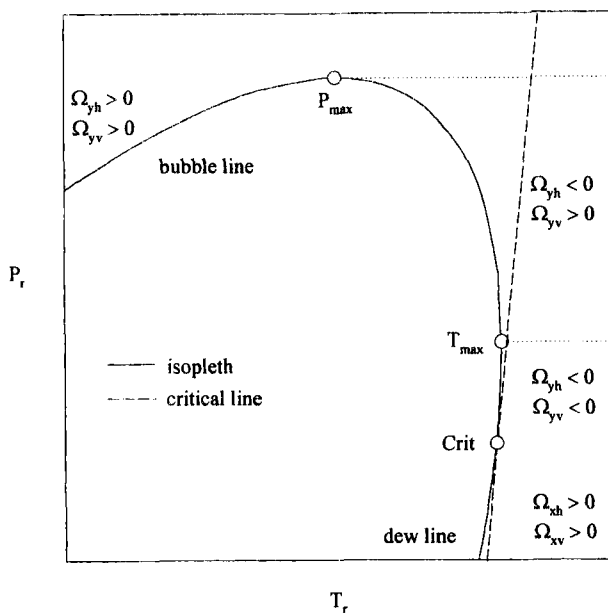


FIGURE 6c Schematic isopleth where the critical point is located below the maximum temperature and the maximum pressure.

partial vaporization volume is generally positive (however, exceptions are clearly shown in the neighborhood of the maximum temperature).

Let us now consider the critical lines 2C' and 2C'' shown in Figure 5d. The geometry of the critical lines suggests a behavior of increasing solubilities in the neighborhood of the critical point 2 (the heavy component) for mixtures diluted in the light component. However, some of supercritical gases such as argon and nitrogen [13] exhibits increasing solubilities in the noncritical ranges of heavy solvents such organic compounds and water. The critical lines and the isopleths of the systems under consideration are not different to the cases illustrated in Figures 6b and 6c in the neighborhood of the critical point of the solvent, which is accessible by mixtures diluted in the light component. The isopleth, as shown in Figures 6b and 6c, is projected with positive Ω_{yh} values from the maximum pressure point. Hence the increasing solubility in non critical ranges is possible when a minimum pressure in the bubble line segment of the isopleth *penetrates* the low pressure range, in order to achieve negative values of Ω_{yh} as

required by Eq. (13). The above discussion will be illustrated with the predictions of the Redlich-Kwong-Soave EOS [16] for the system nitrogen (1) + water (2) [13], considering the interaction parameter k_{ij} zero. Figure 6d shows that at moderate pressures the model predicts qualitatively the increasing solubility of nitrogen with rising temperature (as observed experimentally). Figure 6e shows the corresponding isopleths where a clear minimum value of the pressure is observed along the bubble-point pressure segment; in addition, the minimum penetrates a range of lower equilibrium pressures when lower solubility compositions are considered. Although the Redlich-Kwong-Soave EOS fails to predict gas-gas immiscibility of the second type for this system, where a negative slope of the critical line should be observed, it reproduces correctly the expected behavior of isopleths in the increasing solubility range, generating a minimum value of the pressure in the bubble line segment.

In their present status, modern equations of state can interpolate VLE experimental data of a great variety of mixtures by using special

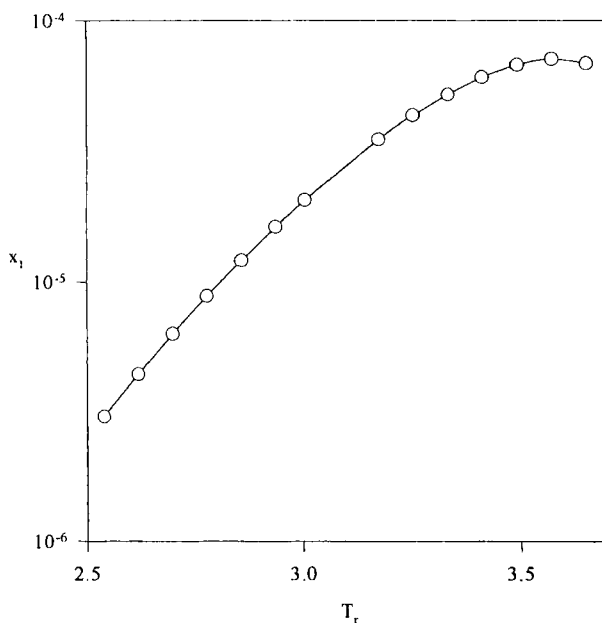


FIGURE 6d Solubility of nitrogen in water at 20 bar, as predicted by the RKS¹⁶ equation ($k_{ij} = 0$).

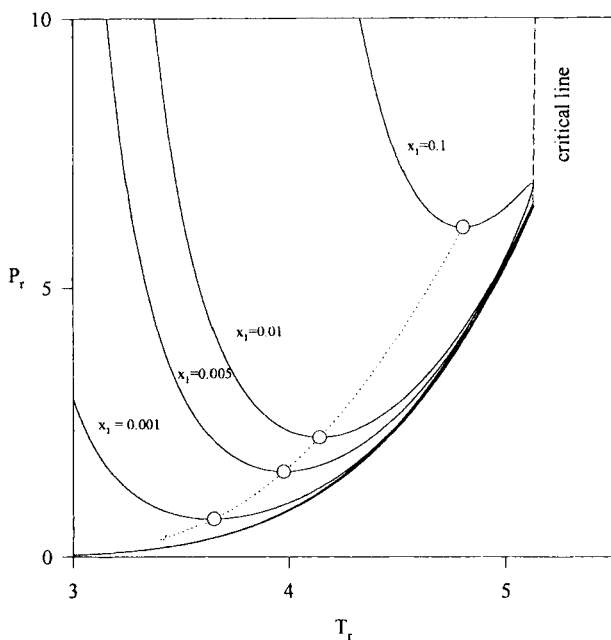


FIGURE 6e Isopleths of the system nitrogen + water in the range of increasing solubilities with rising temperature. Arrows indicate the loci of minimum pressures. Calculations have been done with the RKS¹⁶ equation ($k_{ij} = 0$).

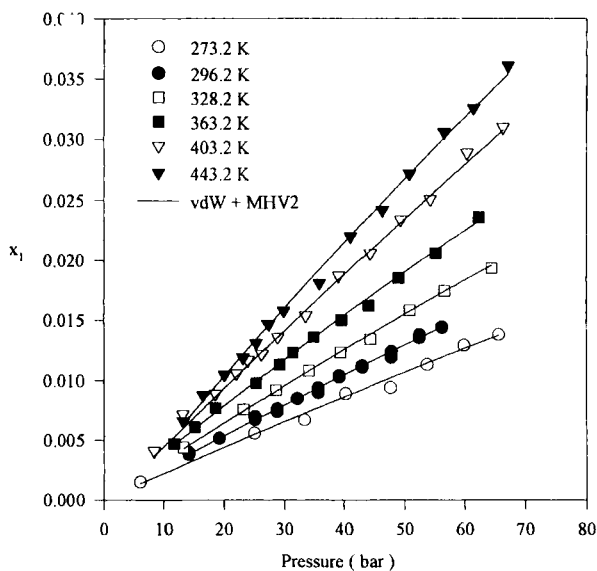


FIGURE 7 Interpolation of the experimental data of the hydrogen (1) - chlorobenzene (2) system using an improved van der Waals EOS. Points indicate the experimental data of Parent and Rempel [18].

mixing rules and functional adaptations for the treatment of quantum gases such as hydrogen [17], and even quantitative results are possible. This point is illustrated in Figure 5 where the the data of Parent and Rempel [18] for the system hydrogen (1) + chlorobenzene (2) have been fitted using the van der Waals EOS, as modified by Soave [19], with the MHV2 mixing rule [20] coupled with the NRTL excess model [21]. As shown by the Figure, the interpolation capability of this particular EOS is excellent.

4. CONCLUSIONS

In this work we have demonstrated that the solubility of gases in liquids can be treated with a complete set of thermodynamical equations and that these can be used to obtain the correct interpretation of the solubility process and the heat effect accompanying it. According to our analysis, the increase of solubility with rising temperature is not restricted to supercritical components only. If azeotropy is present, the most volatile component will become more soluble when the temperature is increased due to an inversion of relative volatilities *instead* of a heat effect. This effect will occur in well defined ranges of compositions that depend on the type of azeotrope (maximum or minimum). When the solubility of a gas in a liquid increases with temperature, the process will be endothermic if the composition of the solvent in the gas phase is negligible and if the supercritical component has a low solubility in the liquid phase. As shown in Appendix A, interpretation of more general cases requires a detailed analysis of the energy balance, in combination with phase equilibrium relationships.

It has also been shown how simple equations of state, in combination with a geometrical interpretation of different projections of phase equilibrium diagrams, can give an explanation of the behavior under consideration. According to our analysis, increasing solubilities of gases for rising temperature conditions will be observed when *the bubble-point pressure segment of an isopleth, will show stationary points in pressure*. The previous discussion *is not model-limited*. Models have been used in our analysis only as a tool for a qualitative prediction of equilibrium lines. The rule given here is a

general rule for isopleths because the analysis has been based on the theory of displacements. Cubic EOS of the van der Waals type are capable of predicting isopleths with multiple extreme points, hence they may be used for fitting solubility data of systems which show an increase in solubility with temperature in binary systems; quantitative agreement may be obtained using advanced mixing rules [17, 22] in complex mixtures.

LIST OF SYMBOLS

- \hat{f}_i = fugacity of component i
 G = Gibbs energy
 G^E = excess Gibbs energy
 H = enthalpy
 n = number of moles
 n_T = total number of moles
 P = absolute pressure
 Q = heat effect in equation (A.6)
 R = universal gas constant
 S = entropy
 T = absolute temperature
 V = volume
 x, y = compositions of the liquid and vapor phases
 z = generic composition

Greek

- $\hat{\phi}$ = fugacity coefficient of component i
 γ = activity coefficient
 μ = chemical potential
 Ψ^L = liquid fraction, defined by equation (A.4)
 Ω_{zm} = sum of the partial vaporization property m weighted in composition z , defined in Eqs. (23) and (24).

Superscripts

- \circ = reference state
 $\hat{}$ = molar property
 $-$ = partial property

- E = excess property
 L = pertaining to the liquid phase
 V = pertaining to the vapor phase

References

- [1] Holmes, L.H. (1996). *J. Chem. Education*, **73**, 143.
- [2] Malesinski, W. (1965). *Azeotropy and Other Theoretical Problems of Vapor Liquid Equilibrium* (Interscience Publishers, London).
- [3] Van Ness, H.C. and Abbott, M.M. (1982). *Classical Thermodynamics of Non-electrolyte Solutions* (McGraw-Hill, New York).
- [4] Kudryavtseva, L.S. and Susarev, M.P. (1963). *Zh. Prikl. Khim.* (Leningrad), **36**, 1231.
- [5] Becker, F. and Hallauer, F. (1988). *Int. DATA Ser., Sel. Data Mixtures, Ser. A*, **16**, 44.
- [6] Morris, J.W., Mulvey, M.M., Abbott, M.M. and Van Ness, H.C. (1975). *J. Chem. Eng. Data*, **20**, 403.
- [7] Larsen, B.L., Rasmussen, P. and Fredenslund, Aa. (1987). *Ind. Eng. Chem. Res.*, **26**, 2274.
- [8] Prausnitz, J.M., Lichtenthaler, R. and Azevedo, E. (1986). *Molecular Thermodynamics of Fluid Phase Equilibria* (Prentice-Hall, New Jersey).
- [9] Van Konynenburg, P.H. and Scott, R.L. (1980). *Phil. Trans. Royal Society (London)*, **298 A**, 495.
- [10] Wild, J.D., Sridhar, H. and Potter, O.E. (1978). *Chem. Eng. J.*, **15**, 209.
- [11] Walas, S. (1985). *Phase Equilibria in Chemical Engineering* (Butterworth, Boston).
- [12] Reid, R., Prausnitz, J.M. and Sherwood, T. (1977). *The Properties of Gases and Liquids*. 3rd. Ed. (McGraw-Hill, New York).
- [13] Schneider, G.M. (1970). *Advan. Chem. Phys.*, **17**, 1.
- [14] Davenport, A.J. and Rowlinson, J.S. (1963). *Trans. Faraday Soc.*, **59**, 78.
- [15] Hicks, C.P. and Young, C.L. (1975). *Chem. Rev.*, **75**(2), 119.
- [16] Soave, G. (1972). *Chem. Engng. Sci.*, **27**, 1197.
- [17] Anderko, A. (1990). *Fluid Phase Equilibria*, **61**, 145.
- [18] Parent, J.S. and Rempel, G.L. (1996). *J. Chem. Eng. Data*, **41**, 192.
- [19] Soave, G. (1984). *Chem. Eng. Sci.*, **39**, 357.
- [20] Dahl, S. and Michelsen, M.L. (1990). *AIChE J.*, **36**, 1829.
- [21] Renon, H. and Prausnitz, J.M. (1968). *AIChE J.*, **14**, 135.
- [22] Wong, D. and Sandler, S. (1992). *AIChE J.*, **38**, 671.

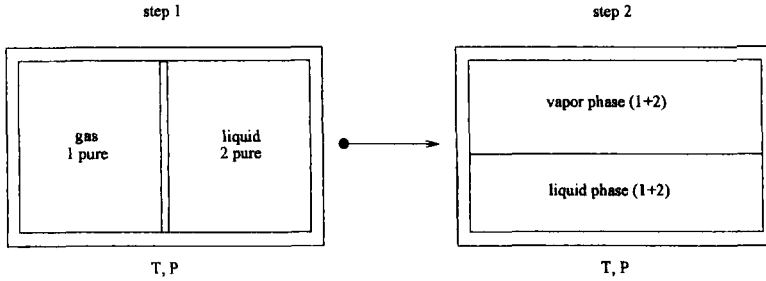
APPENDIX A

Heat effects when a gas is dissolved in a liquid.

The solubility process of a gas (1) in a liquid (2) can be schematically represented as a two step process:

1. Solute and solvent are unmixed in their stable states at the temperature and pressure of the solution.

2. Component 1 and 2 are mixed and the phase equilibrium is achieved



The enthalpy of the initial state is given by

$$H_0 = n_1 \tilde{H}_1^V + n_2 \tilde{H}_2^L = n^T (z_1 \tilde{H}_1^V + z_2 \tilde{H}_2^L) \quad (\text{A.1})$$

and that of the final state

$$H_f = n_1^V \bar{H}_1^V + n_2^V \bar{H}_2^V + n_1^L \bar{H}_1^L + n_2^L \bar{H}_2^L = n^V (y_1 \bar{H}_1^V + y_2 \bar{H}_2^V) + n^L (x_1 \bar{H}_1^L + x_2 \bar{H}_2^L) \quad (\text{A.2})$$

Thus, the solubility heat effect is given by the following energy balance:

$$\begin{aligned} Q &= H_f - H_0 \\ &= n_T [(1 - \Psi^L)(y_1 \bar{H}_1^V + y_2 \bar{H}_2^V) + \Psi^L(x_1 \bar{H}_1^L + x_2 \bar{H}_2^L) - (z_1 \tilde{H}_1^V + z_2 \tilde{H}_2^L)] \end{aligned} \quad (\text{A.3})$$

where Q is the heat effect of the solubilization process and has a positive sign if the process is endothermic and a negative one if the process is exothermic; Ψ^L is the liquid fraction defined as:

$$\Psi^L = \frac{n^L}{n_T} = \frac{n_T - n^V}{n_T} \quad (\text{A.4})$$

From a component material balance we have:

$$z_i = \Psi^L x_i + (1 - \Psi^L) y_i \quad (\text{A.5})$$

It is always possible to find an equilibrium state when $0 < \Psi^L < 1$. Combination of Eq. (A.3) and Eq. (A.5) yields:

$$\frac{Q}{n_T} = \Psi^L \left[\bar{H}_2^L + (\bar{H}_1^L - \bar{H}_1^V + \bar{H}_2^L - \bar{H}_2^V)x_1 - y_2 \bar{H}_2^V - y_1 \bar{H}_1^V \right. \\ \left. + y_1 \bar{H}_1^V - y_1 \bar{H}_2^L \right] + y_1 \bar{H}_1^V + y_2 \bar{H}_2^V - y_1 \bar{H}_1^V - y_2 \bar{H}_2^L \quad (\text{A.6})$$

Equation (A.6) provides a completely general method for the qualification of the heat effect of the solubility process, and should be used in connection with Eq. (14), instead of the Le Châtelier principle. If a nonvolatile solvent is considered and a low solubility of the gas is assumed, then as $x_2 \rightarrow 1, y_2 \rightarrow 0, \bar{H}_2^L \rightarrow \bar{H}_2^L$ and $\bar{H}_1^V \rightarrow \bar{H}_1^V$; thus Eq. (A.6) simplifies to

$$\frac{Q}{n_T} = \Psi^L (\bar{H}_1^L - \bar{H}_1^V)x_1 \approx \Psi^L (\bar{H}_1^L - \bar{H}_1^V)x_1 = -\Psi^L \Delta \bar{H}_1 x_1 \quad (\text{A.7})$$

From Eq. (A.7) it is clear that the heat effect of solubilization has the opposite sign of $\Delta \bar{H}_1$, the partial enthalpy of vaporization, when the indicated assumptions are applicable.

APPENDIX B

Proof: changes of sign of the functions Ω_{2m} for different phases in the neighborhood of the critical point.

The following compositional derivatives, now generalized for phases α and β , can be obtained from Eqs. (8) and (9) (Malesinski [2])

$$\left(\frac{\partial T}{\partial x_1^\alpha} \right)_P = - \frac{T(x_2^\beta - x_2^\alpha)}{x_1^\beta \Delta \bar{H}_1 + x_2^\beta \Delta \bar{H}_2} \left(\frac{\partial^2 \tilde{G}^\alpha}{\partial x_2^{\alpha 2}} \right)_{T,P} \\ = - \frac{T(x_2^\beta - x_2^\alpha)}{\Omega_{x^\beta h}} \left(\frac{\partial^2 \tilde{G}^\alpha}{\partial x_2^{\alpha 2}} \right)_{T,P}$$

$$\left(\frac{\partial T}{\partial x_1^\beta} \right)_P = - \frac{T(x_2^\beta - x_2^\alpha)}{x_1^\alpha \Delta \bar{H}_1 + x_2^\alpha \Delta \bar{H}_2} \left(\frac{\partial^2 \tilde{G}^\beta}{\partial x_2^{\beta 2}} \right)_{T,P} \\ = - \frac{T(x_2^\beta - x_2^\alpha)}{\Omega_{x^\alpha h}} \left(\frac{\partial^2 \tilde{G}^\alpha}{\partial x_2^{\alpha 2}} \right)_{T,P}$$

$$\left(\frac{\partial P}{\partial x_1^\alpha}\right)_T = \frac{x_2^\beta - x_2^\alpha}{x_1^\beta \Delta \bar{V}_1 + x_2^\beta \Delta \bar{H}_2} \left(\frac{\partial^2 \tilde{G}^\alpha}{\partial x_2^{\alpha 2}}\right)_{T,P} = \frac{x_2^\beta - x_2^\alpha}{\Omega_{x^\beta v}} \left(\frac{\partial^2 \tilde{G}^\alpha}{\partial x_2^{\alpha 2}}\right)_{T,P} \quad (\text{B.3})$$

$$\left(\frac{\partial P}{\partial x_1^\beta}\right)_T = \frac{x_2^\beta - x_2^\alpha}{x_1^\alpha \Delta \bar{V}_1 + x_2^\alpha \Delta \bar{V}_2} \left(\frac{\partial^2 \tilde{G}^\beta}{\partial x_2^{\beta 2}}\right)_{T,P} = \frac{x_2^\beta - x_2^\alpha}{\Omega_{x^\alpha v}} \left(\frac{\partial^2 \tilde{G}^\beta}{\partial x_2^{\beta 2}}\right)_{T,P} \quad (\text{B.4})$$

Eqs. (B.1) to (B.4) give the compositional slope of temperature and pressure in binary diagrams $T - x^\alpha - x^\beta$ and $P - x^\alpha - x^\beta$ respectively. It is known that different phases approximate the critical point with compositional slopes of opposite signs, one case is depicted in Figure 5.c where, in the line F-G, the pressure slope is positive for the liquid phase and negative for the vapor phase. Other cases are the upper and lower critical solution temperature in liquid-liquid equilibria. From inspection of Eqs. (B.1) and (B.2), phases can have opposite temperature compositional slope in the neighborhood of the critical if the signs $\Omega_{x^\alpha h}$ and $\Omega_{x^\beta h}$ are opposite. Equivalently, from inspection of Eqs. (B.3) and (B.4), phases can have opposite pressure compositional slope in the neighborhood of the critical if the signs $\Omega_{x^\alpha v}$ and $\Omega_{x^\beta v}$ are opposite.